Continuous sensing of hydrogen peroxide and glucose via quenching of the UV and visible luminescence of ZnO nanoparticles

Article *in* Microchimica Acta · May 2015

DOI: 10.1007/s00604-015-1493-9

CITATIONS
61

READS
564

16 authors, including:

Valerio Beni
Acreo Swedish ICT, Norrkoping, Sweden
66 PUBLICATIONS **1,468** CITATIONS

SEE PROFILE

Anthony P F Turner
Cranfield University
468 PUBLICATIONS **19,607** CITATIONS

SEE PROFILE

Roman Viter
University of Latvia
111 PUBLICATIONS **1,420** CITATIONS

SEE PROFILE

Martin O Eriksson
Linköping University
19 PUBLICATIONS **311** CITATIONS

SEE PROFILE

Microchim Acta (2015) 182:1819–1826
DOI 10.1007/s00604-015-1493-9

ORIGINAL PAPER

Continuous sensing of hydrogen peroxide and glucose via quenching of the UV and visible luminescence of ZnO nanoparticles

Dzmitry Sodzel[1] · Volodymyr Khranovskyy[2] · Valerio Beni[3] · Anthony P. F. Turner[3] · Roman Viter[4,5] · Martin O. Eriksson[2] · Per-Olof Holtz[2] · Jean-Marc Janot[6] · Mikhael Bechelany[6] · Sebastien Balme[6] · Valentyn Smyntyna[5] · Ekaterina Kolesneva[1] · Lyudmila Dubovskaya[1] · Igor Volotovski[1] · Arnolds Ubelis[4] · Rositsa Yakimova[2]

Received: 14 January 2015 / Accepted: 7 April 2015 / Published online: 13 May 2015

Abstract We report on an indirect optical method for the determination of glucose via the detection of hydrogen peroxide (H_2O_2) that is generated during the glucose oxidase (GOx) catalyzed oxidation of glucose. It is based on the finding that the ultraviolet (~374 nm) and visible (~525 nm) photoluminescence of pristine zinc oxide (ZnO) nanoparticles strongly depends on the concentration of H_2O_2 in water solution. Photoluminescence is quenched by up to 90 % at a 100 mM level of H_2O_2. The sensor constructed by immobilizing GOx on ZnO nanoparticles enabled glucose to be continuously monitored in the 10 mM to 130 mM concentration range, and the limit of detection is 10 mM. This enzymatic sensing scheme is supposed to be applicable to monitoring glucose in the food, beverage and fermentation industries. It has a wide scope in that it may be extended to numerous other substrate or enzyme activity assays based on the formation of H_2O_2, and of assays based on the consumption of H_2O_2 by peroxidases.

Keyword Glucose biosensor · Optical assay · Photoluminescence · ZnO · Hydrogen peroxide

✉ Mikhael Bechelany
mikhael.bechelany@univ-montp2.fr

[1] Institute of Biophysics and Cell Engineering of National Academy of Sciences of Belarus, Academicheskaya St. 27, Minsk 220072, Belarus

[2] Department of Physics, Chemistry, and Biology (IFM), Linköping University, 583 81 Linköping, Sweden

[3] Biosensors & Bioelectronics Centre, Linköping University, 583 81 Linköping, Sweden

[4] National Science Center FOTONIKA-LV, University of Latvia, 19, Raina Blvd, 1586 Riga, Latvia

[5] Odessa National I.I. Mechnikov University, 42, Pastera, Odessa 65026, Ukraine

[6] Institut Européen des Membranes, UMR5635 ENSCM UM CNRS, Université Montpellier, 2, Place Eugene Bataillon, 34095 Montpellier cedex 5, France

Introduction

During the last decade considerable attention has been paid to biosensors as new tools for fast, reliable, cost effective and sensitive analysis of clinical, environmental and food samples [1]. Biosensors are specific due to the immobilized biological system used and can therefore detect the smallest amounts of specific substances. Rapid and continuous control is possible with biosensors, and the response time is rather short. One of the most successful applications of biosensors is glucose monitoring, both in medical and food areas. Increasing health-related concerns and growth of the diabetic population are the crucial driving factor for development of glucose biosensors in clinical diagnostics. Monitoring of glucose is also relevant in the food industry, in areas such as food, beverage and fermentation, where the control of this parameter is important in order to ensure the quality of the products.

The first glucose biosensor was described in 1962 by Clark and Lyons [2] as a thin layer of glucose oxidase (GOx) entrapped over an oxygen electrode via a semipermeable dialysis membrane. This first-generation device relied on the use of oxygen as co-substrate, and the production and detection of hydrogen peroxide or the detection of oxygen consumption. The second-generation glucose sensors developed in the early 1980s [3] contained mediators (such as ferrocene or quinones) shuttling electrons from the reduced enzyme to an electrode.

Despite the enormous progress in the field of glucose biosensors during the last decade [4], the majority of the modern glucose biosensors are still of the electrochemical or photoelectrochemical [5, 6] type. This is due to their high sensitivity, reproducibility, and ease of handling as well as their low production and running cost.

Alternative transduction mechanisms, such as using optical signals, [7] are abound in the biosensor literature. In particular, the change in luminescence of upconverting luminescent nanoparticles [8] or a semiconductor can be used as an indicator of the presence of target substances. Ideally, the light intensity should be proportional to the concentration of the analyte of interest. This, however, requires functionalisation of the semiconductor with a biosensitive layer [9], such as an enzyme. Since many enzymes exhibit high specificity for their respective substrates, this type of biosensor can potentially provide ultrahigh selectivity for the target substances.

Basic semiconductor materials have been used previously as transducers for biosensors like Si, SiC, GaN [10] and metal oxide [11]. Among them, zinc oxide (ZnO) can be used, since it has a wide band gap (~3.3 eV) enabling efficient UV luminescence at room temperature [12, 13]. Moreover ZnO has an isoelectric point (pI) as high as ~9.5, which enables efficient immobilization of enzymes with low pI i.e., ≤5 [14]. Additionally, ZnO is biocompatible. Finally, ZnO possesses the largest family of nanostructures, providing high surface-to-volume ratio and high crystalline quality [15–18]. All above listed makes ZnO a promising transducer material for optical biosensors. Particularly, photoluminescence (PL) of ZnO is a distinctive feature that can be used for detection of chemical and biological compounds [15, 19].

The first use of this material in a biosensor was reported by Dorfman et al. when they described the development of a nanoscale ZnO platform that could enhance the detection capability of DNA and protein fluorescence [20]. The ZnO nanoplatform allowed enhanced fluorescence detection of fluorophore-labeled DNA and antibovine IgG when compared to other commonly used substrates. Since then, optical based techniques for biomolecular sensing using ZnO material have grown and found niche applications in immunosorbent assays and disease diagnostics. For instance, immunoassays using bifunctional Fe_3O_4/ZnO/Au nanorices as Raman probes [21] and immunoassays using ZnO quantum dots (QDs) as electrochemical and fluorescent labels [22] have been described. Recently, the fluorescent properties of ZnO QDs have been found useful as probes for ultrasensitive detection of cancer biomarkers [23, 24]. Wang *et al.* developed a surface plasmon resonance based biosensor comprised of ZnO-Au nanocomposites for rabbit IgG detection [25].

Somewhat surprisingly, in spite of the large market size for glucose sensors, implementation of optical schemes for sensing glucose have not been a big success. Taking into account the potential for continuous glucose monitoring using optical methods as well as prospective properties of ZnO material, we report the application of ZnO nanoparticles (NPs) in a biosensor for monitoring glucose at a large concentration range (10 – 300 mM). The biosensor is based on the indirect detection of hydrogen peroxide (H_2O_2) as a product of glucose conversion catalysed by glucose oxidase immobilized on ZnO NPs. The presence of hydrogen peroxide in close proximity with the ZnO NPs causes a respective change of the UV and visible PL signals and therefore can be used for the detection of the glucose concentration in the solution. The continuous sensing of hydrogen peroxide and glucose via quenching of the UV and visible luminescence of ZnO nanoparticles has not been reported before.

Material and methods

Sample preparation

Commercially available low-cost ZnO NPs from Sigma Aldrich (http://www.sigmaaldrich.com) were used as a model transducer material. Prior to use, the NPs were irradiated by UV light in order to convert them into the hydrophilic state and hence make them wettable for the water based solutions [26]. The UV irradiation was realized in air ambient via exposure of the samples, for 30 min, to a low-pressure mercury lamp “Philips TUV PL_L18 W” with a power of 18 W and maximum emission intensity at a wavelength of 254 nm. The biosensitive layer was prepared by physical adsorption of GOx onto the surface of NPs via the following procedure. Firstly, 0.5 mg of ZnO NPs were dispersed in 10 mL of 0. 01 M phosphate buffer. Secondly, the mixture was sonicated for 10 min in order to obtain a homogeneous suspension of nanoparticles. In parallel, the stock solution (10 mg mL^{-1}) of glucose oxidase from *Aspergillus niger* (also purchased from Sigma Aldrich) was prepared. Stock glucose oxidase solution was then added into the ZnO NPs solution resulting in 1 mg mL^{-1} GOx in the mixture. After an incubation period of 2 h under stirred condition, the mixture was centrifuged in order to remove the excess of GOx. Finally, separated ZnO NPs with immobilized GOx were dispersed in 0.01 M phosphate buffer with a pH of 7.0.

Characterization of materials

Prior to immobilization, the morphology of the ZnO NPs was studied by scanning electron microscopy (SEM) using a Leo 1550 Gemini SEM operated with acceleration voltages ranging from 10 to 20 kV and using an aperture value of 30 μm. Photoluminescence spectra were recorded using a spectrometer (Andor Shamrock SR-303i) upon excitation of the NPs solutions with a UV (355 nm) laser.

Change of the PL intensity was monitored by adding 20 μl of hydrogen peroxide and glucose stock solutions of different concentrations into a cuvette with 180 μL of GOx immobilized ZnO NPs mixture (after washing the amount of ZnO NPs was ~10 $\mu g \cdot mL^{-1}$). Initially, 50 μM H_2O_2 was added into the cuvette and the PL emission was measured after 1 min. The procedure was repeated with a certain concentration steps until the peroxide concentration reached 100 mM. Glucose stock solutions were prepared by diluting 3 M glucose (D-(+)-Glucose, Sigma-Aldrich) in 0.01 M phosphate buffer. An initial solution of 0.5 mM glucose was added into the cuvette and 1 min after the addition, the PL from the ZnO NPs was measured. The PL measurements were conducted by adding glucose solutions in a wide range of concentrations up to 300 mM. Control experiments were performed with 20 μl of phosphate buffer instead of glucose or H_2O_2. The PL signal was calculated as the difference of PL intensity maxima at 374 nm (for Near-Band-Edge (NBE)) and 525 nm (for Deep-Level Emission DLE) before and after adding hydrogen peroxide or glucose solutions. Each experiment was repeating five times then we were calculating the average value of PL intensity.

The GOx immobilization mechanism was investigated on flat ZnO surfaces by confocal fluorescence spectroscopy using the set-up described by Ferez et al. [27] et Balme et al. [28]. The ZnO surface was prepared by atomic layer deposition (20 nm thick) on a cover glass using an experimental procedure described by Abou Chaaya et al. [29]. In order to detect adsorbed GOx, the latter was previously labeled using Alexa Fluor 594 succinimidyl ester kit (InvitroGen, A30008; http://www.lifetechnologies.com/). Typically, 500 μL of protein solution was added to dry fluorophore Alexa-594 in a molar ratio of 1:1 and allowed to react for 0.5 h at 20 °C. Then the unreacted Alexa and protein were separated by centrifugation (16,000 g, 15 min) using filter (Biospin P6) according to the supplier of the kit. The labeling ratio [GOx]/[protein] (0.3) was determined from the UV/Vis spectrometry. Interfacial concentration of protein was determined as previously explained by Ferez et al. [27].

Results and discussion

Microstructure and photoluminescence properties of pristine ZnO nanoparticles

Initially, the microstructure of ZnO NPs was studied by SEM (Fig. 1). The NPs were of rather rod shape with uniform size of 70±15 nm and were not agglomerated, which is crucial for their further coating by biological substances. The NPs demonstrated some evidences of hexagonal faceting, reflecting the hexagonal crystal structure of ZnO. The light scattering profiles of the suspension obtained by DLS shows two scattering peaks with maxima at hydrodynamic diameters around 100 and 400 nm respectively (Fig. 1b).

This finding is not surprising since for a non-spherical particle, DLS will give the diameter of a sphere that has the same average translational diffusion coefficient as the particle being measured. Since our ZnO has a rod shape as observed by SEM image (Fig. 1a), the hydrodynamic diameter observed for single nanoparticle is 100 nm. However this finding shows as well that in buffer solution, small agglomerates (peak around 400 nm) formed of 3 to 4 nanoparticles are also observed.

The room temperature photoluminescence (RT PL) spectrum of pristine ZnO NPs is depicted in Fig. 2. The PL spectrum consists of two main peaks: a narrow and intense peak at 384 nm and a wide band of emission, centered at 500 nm. The former is so-called “near band edge” emission (NBE) and it is due to radiative recombination of excited carriers, electrons and holes, in the conduction and valence bands, respectively. While the latter is a defect emission due to radiative recombination of charge carriers at different deep level defect related emission (DLE emission). The structural, optical and electrical properties of ZnO nanostructures are strongly interrelated.

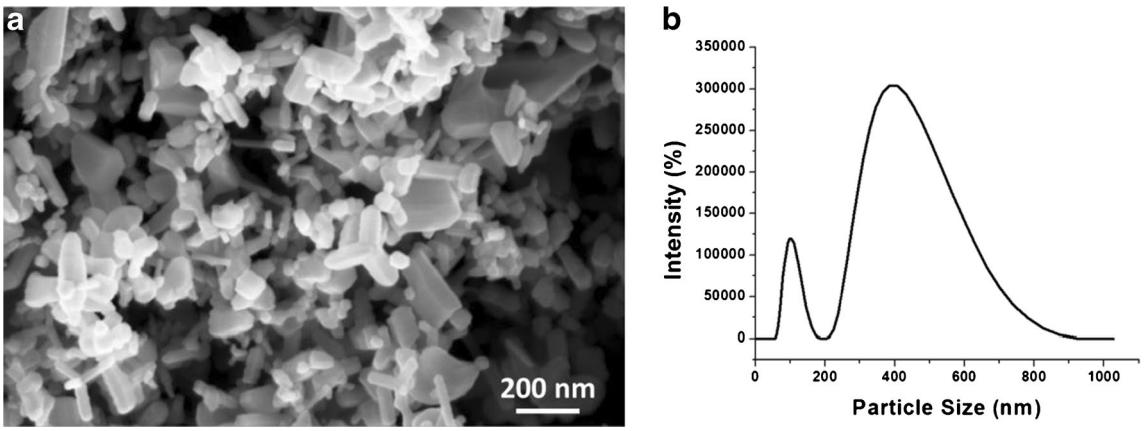

Fig. 1 **a**) SEM image of pristine faceted grains of ZnO NPs agglomerated on the Si surface, and **b**) DLS of dispersion of ZnO nanoparticles in buffer solution

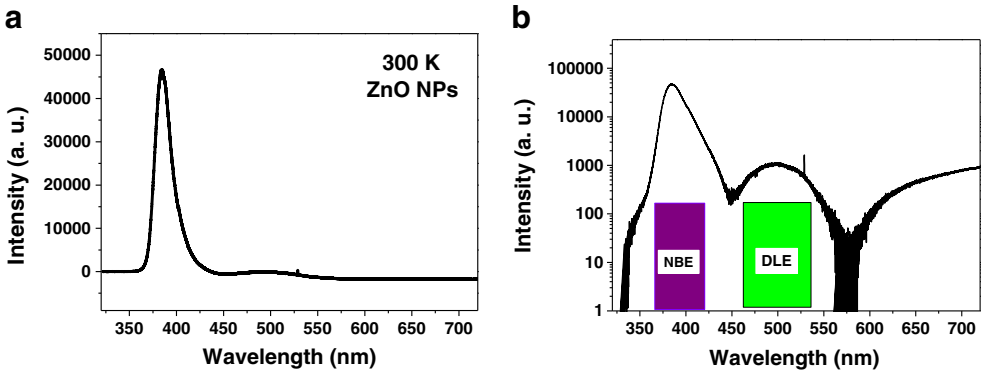

Fig. 2 Room temperature photoluminescence spectra of pristine ZnO NPs, represented in linear (**a**) and logarithmic scale (**b**). Two main emission peaks, Near Band Edge (NBE) and Deep-Level Emission (DLE) emissions are marked in (b)

Usually, the NBE/DLE ratio of ZnO nanostructures increases with improvement of the material stoichiometry [30].

Due to the expected sensing mechanism earlier described by Kim et al. [26], we have initially focused our attention mostly on the NBE emission peak intensity as a useful signal. However, as we have observed further, in our case the intensity of the DLE peak of visible luminescence was also essentially affected by the analyte concentration. Therefore, we considered the change of both peaks intensities (NBE and DLE) separately as a signal for hydrogen peroxide and glucose detection.

Detection of hydrogen peroxide by ZnO NPs photoluminescence

Pristine ZnO NPs were subjected to UV irradiation prior to immobilization of glucose oxidase (GOx). Earlier, it has been reported that wettability character of ZnO can be effectively changed from superhydrophobic to superhydrophilic via irradiation with photons of energies larger than the band gap energy of ZnO [26]. In order to promote better immobilisation of GOx onto ZnO NPs, NPs were UV irradiated for 30 min (see Experimental Section for details). After functionalisation with GOx, the PL of the ZnO NPs was modified with a slight decrease in the signal of both peaks. In order to prove the expected sensing mechanism, the effect of hydrogen peroxide on the PL of ZnO NPs with immobilized GOx was investigated. This was performed by monitoring the PL properties of the NPs upon addition of H_2O_2 in the solution in the range of concentration from 0.05 mM to 100 mM. H_2O_2 was added 12 times into the NPs solutions and the amount of the first addition to the solution was 50 μM. The PL intensity of the ZnO NPs with immobilized GOx was observed to decrease proportionally to the H_2O_2 concentration in the buffer solution.

The PL intensity was demonstrated to decrease in an exponential fashion with H_2O_2 concentration (Fig. 3a). Furthermore, such a decrease was observed for both NBE and DLE peaks even if at different extent. As one can see, the ZnO NPs are very sensitive and concentration of H_2O_2 as low as 0.05 mM could be detected. Such a high sensitivity is presumably due to the large surface area of the NPs. The plots of spectral integral intensity dependencies of the NBE and DLE peaks on the H_2O_2 concentration are plotted in Fig. 3b using a logarithmic scale. As one can see, the DLE emission is an even more efficient spectral characteristic than NBE for

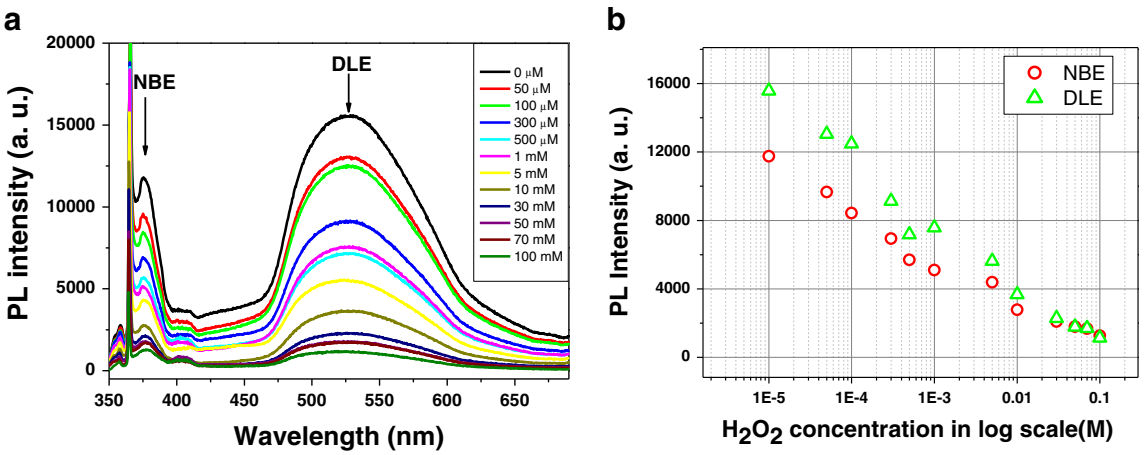

Fig. 3 Dependence of PL spectra of ZnO NPs on the hydrogen peroxide concentration (a) and a logarithmic plot of PL intensity as a function of hydrogen peroxide concentration (b)

H_2O_2 sensing. This can be explained as due to low size of ZnO nanoparticles and therefore the dominant influence of the surface. Hence the deep level defects are mostly localized near the surface and this type of emission is more influenced by H_2O_2 concentration. Here it should be noted that in this specific case, the role of deep level defects is positive, since they provide the independent route to sensitivity via specific luminescence.

The recognition of H_2O_2 can be explained following a collisional quenching mechanism (Fig. 4). Upon excitation, the carriers in ZnO are separated into conduction band (CB - electrons) and valence band (VB - holes). The carriers aim to recombine radiatively while emitting a photon with energy close to the ZnO band gap (~3.3 eV) for NBE emission or alternatively through deep level defects with energies ~2.5 eV for DLE emission. H_2O_2, being in proximity, decomposes catalytically on the ZnO surface into H_2O and O_2. This reaction is followed by acceptance of electrons from the conduction band of ZnO, thus preventing its radiative recombination, and resulting in quenching of the light emission intensity.

GOx surface concentration at equilibrium

Surface adsorption of proteins strongly depends on the surface nature, pH and ionic strength. Thus it is essential to estimate the interfacial concentration of immobilized GOx. To perform this, the latter was adsorbed on ZnO surface prepared by atomic layer deposition and treated with UV light in order to convert it into a hydrophilic state [26]. The interfacial GOx concentration was measured by confocal fluorescence spectroscopy. Typically, 100 nM solution of labeled protein in 0.01 M phosphate buffer at different pH was deposited onto the ZnO surface and the fluorescence from the surface was recorded in real time until equilibrium was attained. Then the surface was then rinsed with buffer solution to remove excess of GOx not bound by electrostatic interaction. The surface concentrations of GOx immobilised at pH 5 and 7 calculated by means of fluorescence intensity at the end of the adsorption process are shown in Fig. 5. As one can see, the amount (149 ng cm^{-2}) of GOx adsorbed on the ZnO surface by immobilization at pH 7 was significantly higher compared to when the

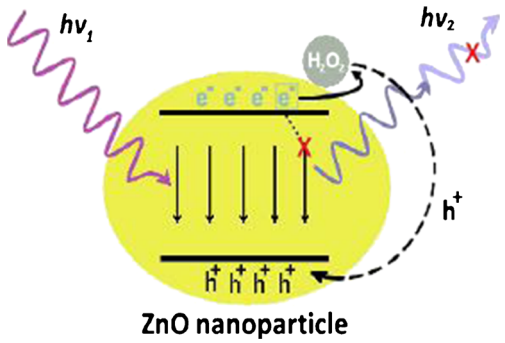

Fig. 4 Suggested mechanism of ZnO NPs PL sensitivity for H_2O_2

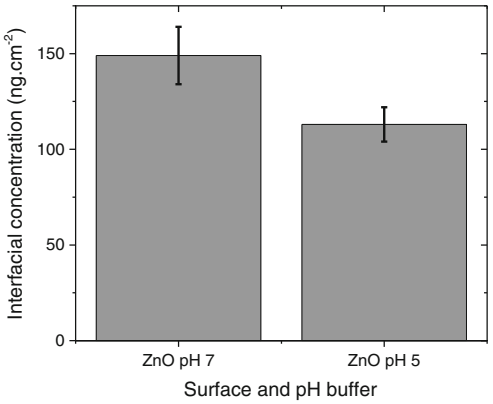

Fig. 5 GOx surface concentration at equilibrium obtained by confocal fluorescence spectroscopy

immobilization was performed at pH 5 (113 ng cm^{-2}). Due to its isoelectric point, ZnO possesses a positive charge at neutral pH, whereas GOx molecules (with low pI 4.2) are negatively charged. This leads to an electrostatic interaction between them and results in their physical binding, and thus effective adsorption.[31] In addition, after rinsing the fluorescence intensity does not decrease which means that the GOx remains on the ZnO surface.

Determination of glucose via quenching of the photoluminescence of ZnO nanoparticles

We employed the mechanism described above for indirect glucose detection. Glucose oxidase was immobilized on ZnO NPs to design a biosensor for glucose control. We have chosen the unspecific adsorption because, it permit to prepare easily our biosensor just before using. Glucose oxidase catalyses the oxidation of the ß-D-glucose to D-glucono-1,5-lactone and hydrogen peroxide. The hydrogen peroxide produced as a result of the glucose conversion enables the detection of the glucose concentration in solution. By measuring the decrease of the PL intensity, one can estimate the glucose concentration in solution. The glucose dissolved in the solution, reacts with the GOx on the surface of ZnO, resulting in gluconic acid and H_2O_2 via the following reaction:

$$\text{D-glucose} + O_2 + H_2O \xrightarrow{\text{GOx}} \text{gluconic acid} + H_2O_2$$

The PL spectra of ZnO NPs with immobilized GOx changed after adding glucose into the solution (Fig. 6a). The figure shows a steady decrease in the PL intensity as the glucose concentration increases. The plot of PL intensity vs. glucose concentration reveals a linear response up to 130 mM as shown in Fig. 6b.

This linear PL intensity decrease is evidence that PL quenching in this system is due to hydrogen peroxide that was produced during the decomposition of glucose molecules

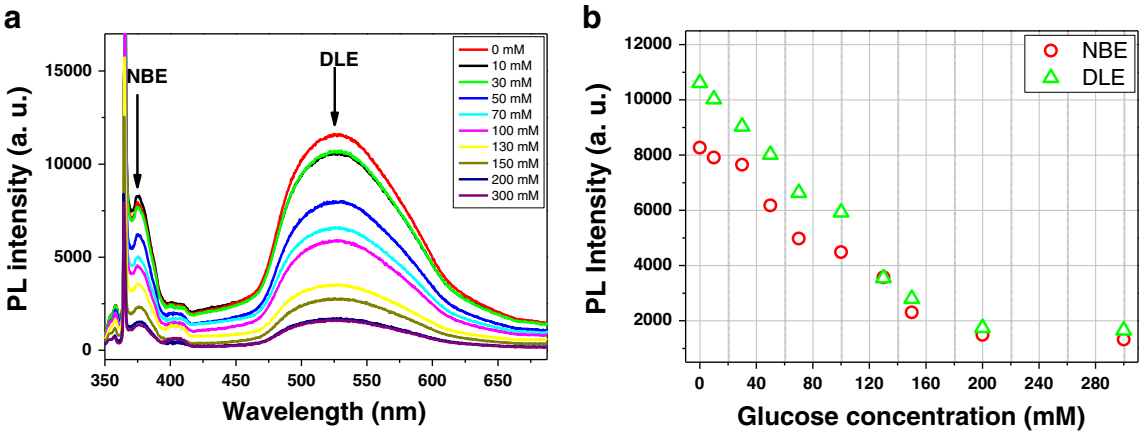

Fig. 6 PL spectra of ZnO NPs at different glucose concentration (**a**); PL intensity vs. glucose concentration (**b**)

on GOx. Electrons from the ZnO nanoparticles excited by UV-light irradiation can transfer to hydrogen peroxide which acts as an electron acceptor quenching the NBE emission.

After the PL intensity testing experiments the sensitivity of the prepared biosensor was estimated over a full range of H_2O_2 and glucose concentrations mentioned before. The PL intensity after reaction of glucose with immobilized GOx was used as a signal for calculation of the sensor response in comparison to the original PL intensity. The sensitivity for H_2O_2 ($S_{H_2O_2}$) and Glucose (S_{Glu}) was calculated as following:

$$S_{H_2O_2} = \frac{I_{\max}^{Gox} - I_{max}^{GOx:H_2O_2}}{I_{\max}^{Gox}}.100\%$$

$$S_{Glu} = \frac{I_{\max}^{Gox} - I_{max}^{GOx:Glu}}{I_{\max}^{Gox}}.100\%$$

where $I_{\max}^{Gox}$ is the spectral intensity of NBE or DLE PL after GOx immobilisation, $I_{max}^{GOx:Glu}$ and $I_{max}^{GOx:Glu}$ are the spectral intensities of NBE or DLE PL after analyte (H_2O_2 and glucose) addition, respectively (Fig. 7).

The intensity of NBE and DLE PL decreased with the increase of both hydrogen peroxide or glucose concentration. The detection threshold for H_2O_2 using NBE and DLE PL was 0.05 mM and the detection limit for glucose was 10 mM using NBE PL. The calibration curve was only near linear at the highest values of glucose concentration (30 mM – 130 mM). The difference of the pure H_2O_2 and glucose sensitivity may be explained as following. First, in case of pure H_2O_2, the PL quenching is due to direct interaction of hydrogen peroxide with ZnO surface, thus the number of radiative recombination acts and thus PL intensity is directly related to the concentration of H_2O_2. In the case of glucose – enzyme – ZnO interaction, only that part of glucose that decomposes on the GO, produces H_2O_2 that participate in the further interaction with ZnO. This explains the difference in dynamic concentrations of glucose and H_2O_2, and thus their difference in PL quenching, and detection limit respectively. Another reason is that GO enzyme, being immobilized on the nanoparticle, cover/shadows part of its active area, thus preventing its contact with hydrogen peroxide as a product of the reaction, thus decreasing the PL quenching and consequently the detection limit. Third, the byproducts of the reaction (gluconic acid) may partially "shadow" the active area of the nanoparticle from the H_2O_2, thus preventing their contact and interaction.

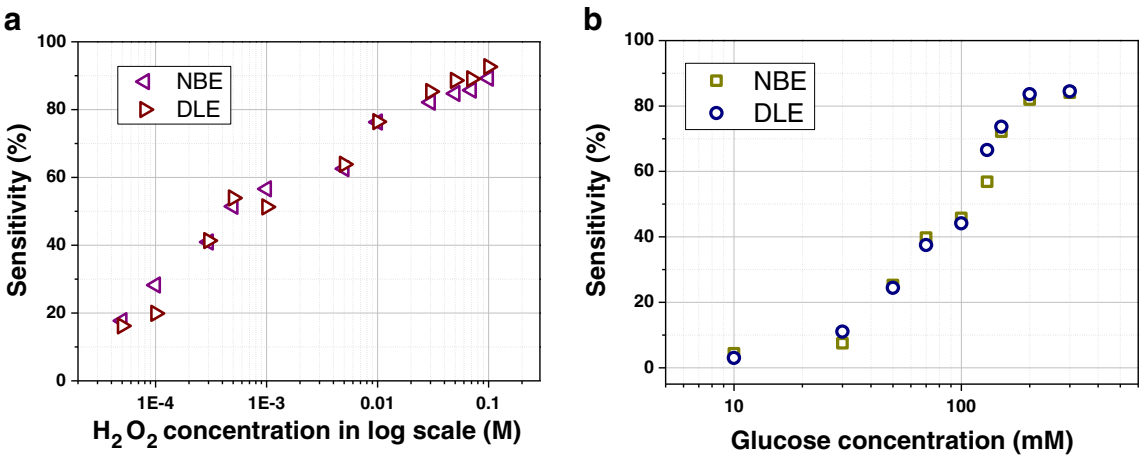

Fig. 7 Sensitivity of the ZnO NP biosensor to H_2O_2 (**a**) and to glucose (**b**) concentrations

The selectivity of our glucose optical sensor depends on two major factors that are the enzyme–analyte reaction and the selective measurements. The enzyme–analyte reaction is very specific due to the nature of the enzyme (Glucose oxidize) functionality. The Glucose oxidize reaction with β-D-glucose is highly specific without any major interfering reaction with other types of sugars.

The selective measurement of the photoluminescence probes technique for the glucose detection has been investigated by Yi et al. [32]. The results clearly demonstrate that the semiconductor based PL sensors can serve as novel fluorescence probes for highly selective and reliable glucose monitoring.

Thus, the detection range of 10 mM to 130 mM of our biosensor covers glucose levels from low to relatively high. It shows potential for the design of optical glucose biosensors for specific applications, including agriculture (i.e., food glucose control) and environmental monitoring.

Therefore, the further improvement of the sensing properties of the studied system can be performed via improvement of the PL ability of ZnO NPs, and optimization of such parameters as the nanoparticles size, dispersion, glucose oxidase immobilization procedure, concentration of immobilized nanoparticles in the solution etc. This, however, represents the future challenges to be solved for the further development of the reported sensing approach.

Conclusion

ZnO NPs demonstrate bright ultraviolet PL at room temperature. Glucose oxidase was demonstrated to be efficiently immobilized on the superhydrophilic surface of ZnO NPs, providing a biosensitive layer for glucose detection. Glucose in solution reacts with GOx and decomposes into H_2O_2 and gluconic acid. Availability of H_2O_2 in close proximity with ZnO NPs surface results in a decrease of NPs PL intensity. This is because H_2O_2 molecules upon decomposition into H_2O and O_2 accept excited electrons from the ZnO conduction band preventing their inter-band recombination with holes in the valence band. The PL quenching was shown to be proportional to the glucose concentration in the solution. The above described concept should be used for the design of optical glucose biosensors, for high concentration glucose detection (upper than 1.8 g L^{-1}) such as addition of glucose syrup in honey [33] or soda analysis [34]. In addition, this concept may be extended to numerous other enzymatic assays based on the formation of H_2O_2 by oxidases or the consumption of H_2O_2 by peroxidases [35–40].

Acknowledgments This work is supported by EC FP-7 IRSES Grant #318520 "Development of nanotechnology based biosensors for agriculture" 2013–2016. Also, the support from the Swedish Research Council (VR) is acknowledged.

References

1. Kirsch J, Siltanen C, Zhou Q, Revzin A, Simonian A (2013) Biosensor technology: recent advances in threat agent detection and medicine. Chem Soc Rev 42:8733–8768
2. Clark LC, Lyons C (1962) Electrode systems for continuous monitoring in cardiovascular surgery. Ann N Y Acad Sci 102:29–45
3. Cass AEG, Davis G, Francis GD, Hill HAO, Aston WJ, Higgins IJ, Plotkin EV, Scott LDL, Turner APF (1984) Ferrocene-mediated enzyme electrode for amperometric determination of glucose. Anal Chem 56:667–671
4. Turner APF (2013) Biosensors: sense and sensibility. Chem Soc Rev 42:3184–3196
5. Li J, Li H, Xue Y, Fang H, Wang W (2014) Facile electrodeposition of environment-friendly Cu2O/ZnO heterojunction for robust photoelectrochemical biosensing. Sensors Actuators B Chem 191: 619–624
6. Xi X, Li J, Wang H, Zhao Q, Li H (2015) Non-enzymatic photoelectrochemical sensing of hydrogen peroxide using hierarchically structured zinc oxide hybridized with graphite-like carbon nitride. Microchim Acta, 1–7
7. Steiner M-S, Duerkop A, Wolfbeis OS (2011) Optical methods for sensing glucose. Chem Soc Rev 40:4805–4839
8. Wilhelm S, del Barrio M, Heiland J, Himmelstoß SF, Galbán J, Wolfbeis OS, Hirsch T (2014) Spectrally matched upconverting luminescent nanoparticles for monitoring enzymatic reactions. ACS Appl Mater Interfaces 6:15427–15433
9. Yakimova R, Selegard L, Khranovskyy V, Pearce R, Spetz AL, Uvdal K (2012) ZnO materials and surface tailoring for biosensing. Frontiers in bioscience (Elite edition) 4:254–78
10. SelegÅrd L, Khranovskyy V, Söderlind F, Vahlberg C, Ahrén M, Käll P-O, Yakimova R, Uvdal K (2010) Biotinylation of ZnO nanoparticles and thin films: a Two-step surface functionalization study. ACS Appl Mater Interfaces 2:2128–2135
11. Shi X, Gu W, Li B, Chen N, Zhao K, Xian Y (2014) Enzymatic biosensors based on the use of metal oxide nanoparticles. Microchim Acta 181:1–22
12. Khranovskyy V, Tsiaoussis I, Yazdi GR, Hultman L, Yakimova R (2010) Heteroepitaxial ZnO nano hexagons on p-type SiC. J Cryst Growth 312:327–332
13. Khranovskyy V, Lazorenko V, Lashkarev G, Yakimova R (2012) Luminescence anisotropy of ZnO microrods. J Lumin 132:2643–2647
14. Wei Y, Li Y, Liu X, Xian Y, Shi G, Jin L (2010) ZnO nanorods/Au hybrid nanocomposites for glucose biosensor. Biosens Bioelectron 26:275–278
15. Khranovskyy V, Yakimova R, Karlsson F, Syed AS, Holtz P-O, Urgessa ZN, Oluwafemi OS, Botha JR (2012) Comparative PL study of individual ZnO nanorods, grown by APMOCVD and CBD techniques. Phys B Condens Matter 407:1538–1542
16. Raghavan R, Bechelany M, Parlinska M, Frey D, Mook WM, Beyer A, Michler J, Utke I (2012) Nanocrystalline-to-amorphous transition in nanolaminates grown by low temperature atomic layer deposition and related mechanical properties. Appl Phys Lett 100, 191912
17. Elias J, Bechelany M, Utke I, Erni R, Hosseini D, Michler J, Philippe L (2012) Urchin-inspired zinc oxide as building blocks for nanostructured solar cells. Nano Energy 1:696–705
18. Chaaya AA, Bechelany M, Balme S, Miele P (2014) ZnO 1D nanostructures designed by combining atomic layer deposition

and electrospinning for UV sensor applications. J Mater Chem A 2: 20650–20658
19. Abou Chaaya A, Viter R, Baleviciute I, Bechelany M, Ramanavicius A, Gertnere Z, Erts D, Smyntyna V, Miele P (2014) Tuning optical properties of Al2O3/ZnO nanolaminates synthesized by atomic layer deposition. J Phys Chem C 118: 3811–3819
20. Dorfman A, Kumar N, Hahm J (2006) Highly sensitive biomolecular fluorescence detection using nanoscale ZnO platforms. Langmuir 22:4890–4895
21. Hong X, Chu X, Zou P, Liu Y, Yang G (2010) Magnetic-field-assisted rapid ultrasensitive immunoassays using Fe3O4/ZnO/Au nanorices as Raman probes. Biosens Bioelectron 26:918–922
22. Gu B, Xu C, Yang C, Liu S, Wang M (2011) ZnO quantum dot labeled immunosensor for carbohydrate antigen 19–9. Biosens Bioelectron 26:2720–2723
23. Somers RC, Bawendi MG, Nocera DG (2007) CdSe nanocrystal based chem-/bio- sensors. Chem Soc Rev 36:579–591
24. Gill R, Zayats M, Willner I (2008) Semiconductor quantum dots for bioanalysis. Angew Chem Int Ed 47:7602–7625
25. Wang L, Sun Y, Wang J, Wang J, Yu A, Zhang H, Song D (2010) Water-soluble ZnO–Au nanocomposite-based probe for enhanced protein detection in a SPR biosensor system. J Colloid Interface Sci 351:392–397
26. Khranovskyy V, Ekblad T, Yakimova R, Hultman L (2012) Surface morphology effects on the light-controlled wettability of ZnO nanostructures. Appl Surf Sci 258:8146–8152
27. Ferez L, Thami T, Akpalo E, Flaud V, Tauk L, Janot J-M, Déjardin P (2011) Interface of covalently bonded phospholipids with a phosphorylcholine head: characterization, protein nonadsorption, and further functionalization. Langmuir 27:11536–11544
28. Balme S, Janot J-M, Déjardin P, Vasina EN, Seta P (2006) Potentialities of confocal fluorescence for investigating protein adsorption on mica and in ultrafiltration membranes. J Membr Sci 284:198–204
29. Abou Chaaya A, Viter R, Bechelany M, Alute Z, Erts D, Zalesskaya A, Kovalevskis K, Rouessac V, Smyntyna V, Miele P (2013) Evolution of microstructure and related optical properties of ZnO grown by atomic layer deposition. Beilstein J Nanotechnol 4:690–698
30. Liao Z-M, Zhang H-Z, Zhou Y-B, Xu J, Zhang J-M, Yu D-P (2008) Surface effects on photoluminescence of single ZnO nanowires. Phys Lett A 372:4505–4509
31. Arya SK, Saha S, Ramirez-Vick JE, Gupta V, Bhansali S, Singh SP (2012) Recent advances in ZnO nanostructures and thin films for biosensor applications: Review. Anal Chim Acta 737:1–21
32. Yi Y, Deng J, Zhang Y, Li H, Yao S (2013) Label-free Si quantum dots as photoluminescence probes for glucose detection. Chem Commun 49:612–614
33. Rodriguez-Saona L E, Allendorf M E (2011) Use of FTIR for Rapid Authentication and Detection of Adulteration of Food. In Annual Review of Food Science and Technology, Vol 2, Doyle M P, Klaenhammer T R, Vol. 2, pp 467–483
34. Scampicchio M, Arecchi A, Lawrence NS, Mannino S (2010) Nylon nanofibrous membrane for mediated glucose biosensing. Sensors Actuators B Chem 145:394–397
35. Schäferling M, Wu M, Wolfbeis O (2004) Time-resolved fluorescent imaging of glucose. J Fluoresc 14:561–568
36. Wolfbeis OS, Schäferling M, Dürkop A (2003) Reversible optical sensor membrane for hydrogen peroxide using an immobilized fluorescent probe, and its application to a glucose biosensor. Microchim Acta 143:221–227
37. Wolfbeis OS, Dürkop A, Wu M, Lin Z (2002) A europium-Ion-based luminescent sensing probe for hydrogen peroxide. Angew Chem Int Ed 41:4495–4498
38. Wu M, Lin Z, Wolfbeis OS (2003) Determination of the activity of catalase using a europium (III)–tetracycline-derived fluorescent substrate. Anal Biochem 320:129–135
39. Lin Z, Wu M, Wolfbeis OS, Schäferling M (2006) A novel method for time-resolved fluorimetric determination and imaging of the activity of peroxidase, and its application to an enzyme-linked immunosorbent assay. Chem Eur J 12:2730–2738
40. Wu M, Lin Z, Schäferling M, Dürkop A, Wolfbeis OS (2005) Fluorescence imaging of the activity of glucose oxidase using a hydrogen-peroxide-sensitive europium probe. Anal Biochem 340: 66–73